

Optimal Direct Torque Control of Three-Phase Symmetric Induction Motors

Georgios Papafotiou, Tobias Geyer and Manfred Morari

Abstract—Direct Torque Control (DTC) is a state of the art control methodology for induction motor drives which features very favorable control performance and implementation properties. However, one of its main deficiencies is the lack of a systematic design procedure for the inverter switching table, which is the core of the control system. This is addressed in this paper, where we propose a novel modelling and control approach for the DTC problem which is based on a systematic design procedure. The DTC drive comprising of a three-level dc-link inverter driving a three-phase induction motor is modelled in the hybrid Mixed Logical Dynamical (MLD) framework, and a constrained optimal control problem is set up and solved over a receding finite horizon using Model Predictive Control (MPC). Simulation results are provided and compared to the current industrial state of the art, which demonstrate the potential for performance improvements.

I. INTRODUCTION

During the last decades, the rapid development of power semiconductor devices has led to the increased use of adjustable speed induction motor drives in a variety of applications. One of the various methods that are used for controlling the induction motor's torque and speed in such systems is Direct Torque Control (DTC), which was introduced in 1985 by Takahashi and Noguchi [1] and is nowadays a well established industrial standard for induction motor drives [2]. The basic principle of DTC is to exploit the fast stator flux dynamics and to directly manipulate the stator flux vector such that the desired torque is produced. This is achieved by choosing an inverter switch combination that drives the stator flux vector to the desired position by directly applying the appropriate voltages to the motor windings. This choice is made usually every $25 \mu\text{s}$ using a pre-designed switching table that is derived in a heuristic way.

Motivated by the lack of a systematic design procedure for the switching table, a novel approach to the DTC problem of three-phase induction motors is presented in this paper, aiming at making the design process independent of the drive's characteristics and specifications. The DTC drive is modelled as a hybrid system where the inverter switch positions are represented by integer variables. Nonlinearities are approximated by piecewise affine (PWA) functions, and the complete system including constraints is described in the Mixed Logic Dynamic (MLD) framework [3]. Based on the derived hybrid model, a receding horizon constrained finite-time optimal control problem is set up and solved. More

The authors are with the Automatic Control Laboratory, ETH Zentrum – ETL, Swiss Federal Institute of Technology, CH-8092 Zürich, Switzerland
papafotiou,geyer,morari@control.ee.ethz.ch

specifically, the control strategy used is *Model Predictive Control* (MPC) which, as introduced in [4], is well suited for the constrained optimal control of hybrid systems described in the MLD framework. The control objectives are directly expressed in an objective function, and the control law is obtained by minimizing it subject to the MLD model and the physical constraints. As we use the 1-norm, this minimization problem leads to a *Mixed-Integer Linear Program* (MILP) which can be solved efficiently using off-the-shelf solvers. We will refer to this approach as *Optimal DTC*.

The problem considered is based on ABB's ACS6000 DTC drive [5] using a squirrel-cage rotor induction motor with a rated apparent power of 2 MVA and a 3.3 kV three-level dc-link inverter. The performance of the Optimal DTC scheme is evaluated through simulations solving the optimal control problem on-line. The simulations were carried out using the Matlab/Simulink model of the drive provided by ABB. Furthermore, the simulation results of the Optimal DTC were compared to the ones of ABB's DTC strategy.

The paper is organized in the following way. The basic terminology is introduced in Section II. In Section III the hybrid model of the DTC drive is presented, and in Section IV the optimal control problem is formulated followed by simulation results in Section V. Section VI concludes the paper with a summary and an outlook.

Throughout the paper, we will use a normalized time scale t with 1 time unit corresponding to $1/\omega_b$ seconds, where ω_b is the base angular velocity used to calculate the inductive reactances of the motor. Additionally, we will use $x(t)$, $t \in \mathbb{R}$, to denote continuous-time variables, and $x(k)$, $k \in \mathbb{N}$, to denote discrete-time variables with the sampling time T_s . Furthermore, the state estimation of the motor is considered to be ideal. An extended version of this paper is available in [6].

II. PRELIMINARIES

A. The $dq0$ Reference Frame

For the modelling of the DTC drive, all variables are transformed from the three-phase system (abc) to an orthogonal $dq0$ reference frame with a direct (d), a quadrature (q) and a zero (0) axis, that can be either stationary or rotating. Details regarding reference frame theory can be found in the relevant literature [7]. For the needs of this paper, the transformation of a vector $\xi_{abc} = [\xi_a \ \xi_b \ \xi_c]^T$ from the three-phase system to the vector $\xi_{dq0} = [\xi_d \ \xi_q \ \xi_0]^T$ in the

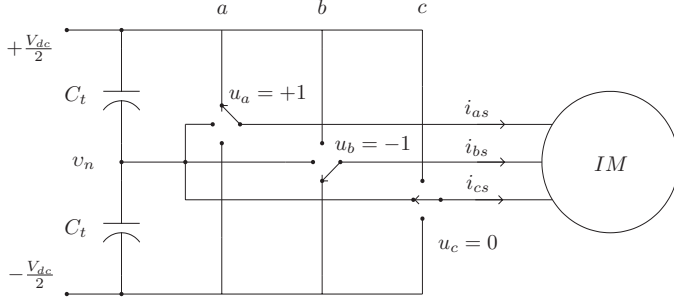


Fig. 1. The equivalent representation of a three-phase three-level inverter driving an induction motor

dq0 frame is carried out through

$$\xi_{dq0} = \mathbf{P}(\varphi)\xi_{abc}, \quad (1)$$

where φ is the angle between the a-axis of the three-phase system and the d-axis of the reference frame, and

$$\mathbf{P}(\varphi) = \sqrt{\frac{2}{3}} \begin{bmatrix} \cos \varphi & \cos(\varphi - \frac{2\pi}{3}) & \cos(\varphi + \frac{2\pi}{3}) \\ -\sin \varphi & -\sin(\varphi - \frac{2\pi}{3}) & -\sin(\varphi + \frac{2\pi}{3}) \\ \frac{\sqrt{2}}{2} & \frac{\sqrt{2}}{2} & \frac{\sqrt{2}}{2} \end{bmatrix}. \quad (2)$$

If the frame is rotating with the angular speed ω_{fr} , then $\varphi = \omega_{fr}t + \varphi_0$, otherwise, if the frame is stationary, φ is time-invariant. Note that the selected transformation matrix is orthonormal, i.e.

$$\mathbf{P}(\varphi)\mathbf{P}^T(\varphi) = \mathbf{I}. \quad (3)$$

B. Model of the Three-level Inverter

An equivalent representation of a three-phase three-level inverter driving an induction motor is shown in Fig. 1. At each phase, the inverter can produce the three different voltages $-\frac{V_{dc}}{2}, 0, \frac{V_{dc}}{2}$, where V_{dc} denotes the voltage of the dc-link. The switch positions of the inverter can therefore be fully described using the three integer variables $u_a, u_b, u_c \in \{-1, 0, 1\}$, where each variable corresponds to one phase of the inverter, and the values $-1, 0, 1$ correspond to the phase potentials $-\frac{V_{dc}}{2}, 0, \frac{V_{dc}}{2}$, respectively.

There are 27 different vectors of the form $\mathbf{u}_{abc} = [u_a \ u_b \ u_c]^T$, that comprise the integer variables describing the inverter. Using the relation (1), these can be transformed into the dq0 frame resulting in vectors of the form $\mathbf{u}_{dq0} = [u_d \ u_q \ u_0]^T$. The latter are shown in Fig. 2 where they are mapped in the two-dimensional dq plane. Even though they are commonly referred to as voltage vectors, this term describes the switch positions rather than the actual voltages applied to the machine terminals.

When operating a three-level inverter, the neutral point potential and the smooth distribution of the switching effort between the upper and the lower half of the inverter deserve particular attention. As can be seen in Fig. 1, the neutral point potential is only affected if one of the voltage vector components is zero. Introducing the real state v_n , the neutral

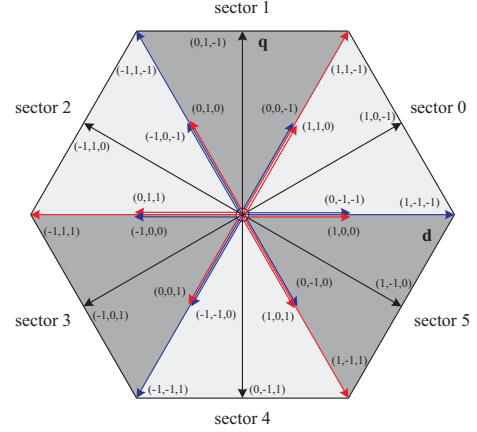


Fig. 2. The voltage vectors on the dq plane and the corresponding values of the integer variables that produce them

point potential is described in continuous-time by

$$\frac{dv_n}{dt} = -\frac{1}{2x_c} [(1 - |u_a|)i_{as} + (1 - |u_b|)i_{bs} + (1 - |u_c|)i_{cs}], \quad (4)$$

with i_{as}, i_{bs}, i_{cs} being the phase stator currents and x_c one of the two symmetric capacitors of the dc-link in p.u.. By transforming the vectors to the dq0 frame and taking advantage of (3), it is straightforward to derive

$$\frac{dv_n}{dt} = \frac{1}{2x_c} \mathbf{u}_{|dq0|}^T \mathbf{i}_{s,dq0}, \quad (5)$$

where $\mathbf{i}_{s,dq0}$ is the stator current expressed in the dq0 frame, and $\mathbf{u}_{|dq0|}$ is the transformation of the vector $|\mathbf{u}_{abc}| = [|u_a| \ |u_b| \ |u_c|]^T$. Note that the absolute value is defined componentwise. For more details about the nature of the neutral point potential and the related balancing problem the reader is referred to [8].

Distributing the switching losses evenly between the semiconductor devices is essential for the inverter's operation, since it helps to prevent that some devices are overloaded while others remain under-utilized. Such phenomena are especially likely at low frequencies (below 50% of the nominal), and can have obvious negative effects on the inverter's life. Here, we approximate the problem by considering the distribution of the switching effort between the upper and the lower half of the inverter using the integer state λ . In discrete-time, the distribution of the switching effort is given by

$$\lambda(k+1) = \lambda(k) + u_a(k) + u_b(k) + u_c(k). \quad (6)$$

It is straightforward to see that if λ becomes too positive (negative), the upper (lower) inverter half is excessively used.

C. Model of the Induction Motor

The dynamics of the squirrel-cage rotor induction motor are modelled in the dq0 reference frame that is rotating synchronously with the rotor with the angular speed ω_r . The d- and q-components of the stator and rotor flux linkages

per second ψ_{ds} , ψ_{qs} , ψ_{dr} and ψ_{qr} , respectively, and the rotor's rotational speed ω_r are used as state variables. The 0-axis components are neglected, since they do not contribute to the electromagnetic torque and are decoupled from the dynamics in the d- and q-axis. The input voltages v_{ds} and v_{qs} are the transformation of the voltages applied to the stator into the dq0 frame. The model parameters are the base angular velocity ω_b , the stator and rotor resistances r_s and r_r , the stator, rotor and mutual inductive reactances x_{ls} , x_{lr} and x_m , respectively, the inertia constant H expressed in seconds, and the mechanical load torque T_ℓ . Note that throughout this paper if not otherwise stated, we are using normalized quantities, and the rotor quantities are referred to the stator circuit.

In this standard dynamical model of the induction motor, the saturation of the machines magnetic material, the changes of the rotor resistance due to the skin effect, and the temperature changes of the stator resistance are ignored. A more elaborate presentation of the induction motors modelling procedure is out of the scope of this paper, and the reader is referred to [7] for details. The induction motor dynamics can be classified into three groups with regard to their time constants. The mechanical part of the motor, in particular the rotational speed, feature time constants in the range of seconds, depending on the load conditions. The rotor fluxes have a typical rotor time constant ranging around 100-200 ms. Finally, the stator flux presents the fastest dynamics, and can be manipulated by the applied stator voltage within a few μ s.

III. LOW COMPLEXITY DISCRETE-TIME MODELLING

A. Symmetrical Properties of the System

The voltage vectors that can be produced by a three-level inverter exhibit strong symmetrical properties on the dq plane. As shown in Fig. 2, a certain pattern is repeated with an angle spread of $\frac{\pi}{3}$. Defining such a pattern as a sector leads to the formation of 6 sectors. On the dq plane, rotating any sector by $\frac{\pi}{3}$ yields the vectors of the neighboring sector. This does not hold for the dq0 space, however, where the corresponding voltage vectors of neighboring sectors have opposite zero components [6].

B. Stator Flux Dynamics Model

In order to derive a low-complexity model of the induction motor that is suitable for the optimal control problem formulation, two basic characteristics of DTC have to be taken into account. Firstly, the stator flux dynamics are significantly faster than the dynamics of the rotor flux and the rotational speed. Thus, the application of a certain voltage vector to the machine terminals has an immediate effect only on the stator flux, turning it rapidly to the position required by the torque demand, while the rotor speed ω_r and the *length* of the rotor flux vector remain constant during several control cycles.

The second characteristic is that the control objectives concerning the motor, namely the maintenance of the length

of the stator flux vector and the electromagnetic torque within the specified bounds, are only affected by the relative (and not the absolute) position of the stator and rotor flux vectors. This is because the electromagnetic torque is the external product of these two vectors. Exploiting the symmetrical properties of the voltage vectors, it is sufficient to map the fluxes into the 0 sector, to solve the control problem in this sector, and to subsequently rotate the result back into the original sector yielding the voltage vector to be actually applied to the motor terminals.

The rotation of the flux vectors can be carried out in two stages. The first stage maps the problem into the 0 sector by rotating the flux vectors clockwise by an integer multiple of $\frac{\pi}{3}$, whereas the second stage is an anti-clockwise rotation of the reference frame by an angle $\varphi \in [0, \frac{\pi}{3}]$, that aligns the rotor flux vector with the d-axis of the reference frame. Assume that the rotor flux initially lies in sector ν . Rotating the fluxes by the angle $\vartheta = \frac{\nu\pi}{3} + \varphi$ yields the rotated flux vectors which are defined as

$$\boldsymbol{\psi}_s^\vartheta = [\psi_{ds}^\vartheta \quad \psi_{qs}^\vartheta]^T, \quad \boldsymbol{\psi}_r^\vartheta = [\psi_{dr}^\vartheta \quad \psi_{qr}^\vartheta]^T. \quad (7)$$

Given the fact that this rotation aligns the rotor flux vector with the d-axis of the rotating frame, and recalling the slow dynamics of the rotor flux vector, one introduces only a negligible error by assuming that ψ_{dr}^ϑ is constant and $\psi_{qr}^\vartheta = 0$ during several sampling intervals. Since the rotational speed dynamics are even slower, also ω_r remains constant. Defining the matrix

$$\mathbf{F} = \begin{bmatrix} -r_s \frac{x_m + x_{lr}}{D} & \omega_r \\ -\omega_r & -r_s \frac{x_m + x_{lr}}{D} \end{bmatrix}, \quad (8)$$

where $D = (x_{ls} + x_m)(x_{lr} + x_m) - x_m^2$, the stator flux dynamics can be described using a reference frame that is rotating synchronously with the rotor by a set of affine state equations

$$\frac{d\boldsymbol{\psi}_s^\vartheta(t)}{dt} = \mathbf{F}\boldsymbol{\psi}_s^\vartheta(t) + r_s \frac{x_m}{D} \boldsymbol{\psi}_r^\vartheta + \frac{V_{dc}}{2} \mathbf{P}(\varphi(k)) \mathbf{u}_{abc}(t),$$

that regard ω_r and ψ_{dr}^ϑ as parameters. To derive the discrete-time mapping of the stator fluxes from the beginning of the sampling interval to its end, note that the voltage vector applied to the motor terminals remains constant within one sampling interval. The discrete-time model of the stator flux dynamics is then obtained by solving (9) from $t = kT_s$ to $t = (k+1)T_s$. Note that the matrix $\mathbf{P}(\varphi(k))$ performing the transformation of the inverter voltages into the rotating dq0 frame is time-varying. In particular, it depends on the angle φ

$$\varphi(k+1) = \varphi(k) + \omega_r T_s, \quad (9)$$

that captures the evolution of the rotating reference frame. The two outputs of the model are the electromagnetic torque

$$T_e(k) = \frac{2}{3} \frac{x_m}{D} \psi_{dr}^\vartheta \psi_{qs}^\vartheta(k), \quad (10)$$

that is a linear expression of the second state, and the length of the stator flux vector

$$\Psi_s(k) = \sqrt{(\psi_{ds}^\vartheta(k))^2 + (\psi_{qs}^\vartheta(k))^2}, \quad (11)$$

that is nonlinear in the first two states.

C. Discrete-time Model of the Three-level Inverter

The neutral point potential in continuous-time is described by (5), and depends on $\mathbf{u}_{|dq0|}$ and $\mathbf{i}_{s,dq0}$. The d- and q-components of the stator current $\mathbf{i}_{s,dq0}$ are linear combinations of the d- and q-components of the stator and rotor flux vectors, and the 0-component is always zero¹.

$$\mathbf{i}_{s,dq0} = \left[\frac{x_{rr}}{D} \boldsymbol{\psi}_s^T - \frac{x_{m}}{D} \boldsymbol{\psi}_r^T \quad 0 \right]^T. \quad (12)$$

Recalling that the fluxes initially lie in the ν sector, and since the optimal control problem will be formulated and solved in the 0 sector, the obtained voltage vector has to be rotated back into the ν sector. Nevertheless, a voltage vector in the 0 sector and its corresponding vectors in the even sectors have the same componentwise absolute vectors. On the other hand, a voltage vector in the 0 sector and its equivalents in the odd sectors have opposite componentwise absolute vectors. Therefore, (5) can be written in discrete-time as

$$v_n(k+1) = v_n(k) + (-1)^\nu \frac{T_s}{2x_c} \mathbf{u}_{|dq0|}^T(k) \mathbf{i}_{s,dq0}(k), \quad (13)$$

where $(-1)^\nu$ accounts for the above property of the componentwise absolute voltage vectors, as detailed in [6]. A similar observation holds for the distribution of the switching losses. Here, a correction term distinguishing between even and odd sectors is also needed, and (6) is rewritten as

$$\lambda(k+1) = \lambda(k) + (-1)^\nu (u_a(k) + u_b(k) + u_c(k)). \quad (14)$$

D. Hybrid Model of the DTC Drive

The overall MLD [3] model of the DTC drive includes the two submodels of the induction motor and the three-level inverter. The motor state equations of the stator flux are given by the discrete-time representation of (9). One state is needed to evaluate the time-varying matrix $\mathbf{P}(\varphi(k))$. Rather than introducing $\varphi(k)$, we choose $\cos(\varphi(k))$ as the third real state as this proves to be beneficial in terms of the model complexity as detailed in [6]. The corresponding state equation is

$$\alpha(k+1) = \cos(\omega_r T_s) \alpha(k) - \sin(\omega_r T_s) \beta(k), \quad (15)$$

where

$$\alpha(k) = \cos(\varphi(k)), \quad \beta(k) = \sin(\varphi(k)). \quad (16)$$

The inverter adds the two state equations (13) and (14). The overall state vector is

$$\mathbf{x}(k) = [\psi_{ds}^\vartheta(k) \quad \psi_{qs}^\vartheta(k) \quad \alpha(k) \quad v_n(k) \quad \lambda(k)]^T. \quad (17)$$

¹This follows from (1), taking into account that $i_{as} + i_{bs} + i_{cs} = 0$.

The model outputs are the electromagnetic torque T_e , and the length of the stator flux vector Ψ_s amounting to the output vector

$$\mathbf{y}(k) = [T_e(k) \quad \Psi_s(k)]^T. \quad (18)$$

The model inputs are the integer variables u_a , u_b and u_c

$$\mathbf{u}(k) = [u_a(k) \quad u_b(k) \quad u_c(k)]^T. \quad (19)$$

The model of the DTC drive contains several nonlinearities, namely the two multiplications in the state equation (13) of the neutral point potential, the computation (11) of the length of the stator flux vector, and the matrix $\mathbf{P}(\varphi(k))$ with the components $\sin(\varphi(k))$ and $\cos(\varphi(k))$. As the MLD framework does not allow to directly describe general nonlinear functions, they need to be approximated by PWA functions. As we have chosen $\alpha(k) = \cos(\varphi(k))$ as a real state, we approximate $\beta(k)$ as a function of $\alpha(k)$. The number of regions that is selected for these approximations results from a trade-off between the required model accuracy and the increase in the complexity of the MLD model. For the problem considered here, the maximum approximation error introduced was chosen to be smaller than 0.5%. The above procedure yields an MLD system with 5 states, 87 z -variables, 55 δ -variables and 443 inequality constraints [6].

IV. OPTIMAL DIRECT TORQUE CONTROL

In the sequel, we propose a new Optimal DTC scheme that replaces the heuristically designed switching table and not only leads to a systematic design procedure, but also improves the performance of the currently employed industrial DTC. Our controller is based on optimal control with a receding horizon policy, more specifically on Model Predictive Control (MPC). Next, we formulate the control objectives which can be classified in three priority levels. The main objectives are to keep the torque and the amplitude of the stator flux within the pre-specified bounds, and to also retain the neutral point potential within bounds that are typically symmetric around zero. As these bounds shall not be violated, we assign to these objectives the highest priority, and express them in the objective function by introducing soft constraints which reflect the bounds.

The control objective with secondary priority is to minimize the average switching frequency. This is equivalent to minimize the number of switch *transitions* within the prediction interval. Due to the limited length of the prediction interval, one needs to enforce that switch transitions are only performed if absolutely necessary, i.e. when refraining from switching would lead to a violation of the bounds on the controlled variables within one time-step. This leads to what we call the *Late Switching Strategy*, where the controller postpones any scheduled switch transition until absolutely necessary. This strategy is implemented by associating a time-decaying penalty with the switch transitions, where switch transitions within the first time-step of the prediction interval result in larger penalties than those that are far in the future.

In particular for short prediction intervals, for a given state, two or more control moves may have the same associated costs according to the two penalty levels introduced above. In the presence of such ambiguities, the control move is preferable the one that moves some of the controlled variables closest to their references, in particular the stator flux and the neutral point potential. We account for that by adding a third, low priority penalty level on the deviation of the stator flux and the neutral point potential from their respective references. For the torque, however, it is preferable to take full advantage of the window width. Thus we refrain from adding such a penalty term to the torque. Another objective of low priority is to distribute the switching effort evenly between the upper and lower half of the inverter. We account for that by adding a small penalty on the distribution of the switching effort.

Based on the controller objectives, we establish next the mathematical expression of the objective function, that is composed of a number of cost expressions. The soft constraints on the upper and lower torque bounds $T_{e,max}$ and $T_{e,min}$, respectively, lead for the electromagnetic torque to the cost expression

$$\varepsilon_T(k) = \begin{cases} q_T(T_e(k) - T_{e,max}) & \text{if } T_e(k) \geq T_{e,max} \\ q_T(T_{e,min} - T_e(k)) & \text{if } T_e(k) \leq T_{e,min} \\ 0 & \text{else,} \end{cases} \quad (20)$$

where $q_T \gg 0$ is the weight on the soft constraints. The cost expression for the length of the stator flux vector is defined similarly using the upper and lower flux bounds $\Psi_{s,max}$ and $\Psi_{s,min}$, respectively, with an additional term penalizing the deviation from the reference $\Psi_{s,ref}$

$$\varepsilon_\Psi(k) = \begin{cases} q_F(\Psi_s(k) - \Psi_{s,max}) & \text{if } \Psi_s(k) \geq \Psi_{s,max} \\ q_F(\Psi_{s,min} - \Psi_s(k)) & \text{if } \Psi_s(k) \leq \Psi_{s,min} \\ q_f|\Psi_s(k) - \Psi_{s,ref}| & \text{else,} \end{cases} \quad (21)$$

with the weights q_F and q_f , $q_F \gg q_f > 0$, on the soft constraints and on the deviation from the reference, respectively. For the neutral point potential, the cost $\varepsilon_v(k)$ is defined according to (21) with the respective bounds $v_{n,max}$ and $v_{n,min}$, the reference 0, and the weights q_N and q_n . The distribution of the switching effort has the simple cost

$$\varepsilon_\lambda(k) = q_\lambda|\lambda(k) - 0| \quad (22)$$

with $q_\lambda > 0$. The switch transitions are penalized using a time-varying weight $q_u(k) > 0$ and the 1-norm

$$\varepsilon_u(k) = q_u(k)\|\mathbf{u}(k) - \mathbf{u}(k-1)\|_1. \quad (23)$$

Define the vector $\varepsilon = [\varepsilon_T \ \varepsilon_\Psi \ \varepsilon_v \ \varepsilon_\lambda \ \varepsilon_u]^T$ and consider the objective function

$$J(\mathbf{U}(k), \mathbf{x}(k), \mathbf{u}(k-1)) = \sum_{\ell=0}^{N-1} \|\varepsilon(k+\ell|k)\|_1 \quad (24)$$

which penalizes the predicted evolution of $\varepsilon(k+\ell|k)$ from the time-instant k on over the finite horizon N using the 1-norm. The control law at time-instant k is then obtained by

minimizing the objective function (24) over the sequence of control moves $\mathbf{U}(k) = [\mathbf{u}(k), \dots, \mathbf{u}(k+N-1)]^T$ subject to the evolution of the MLD model and its mixed-integer linear inequality constraint, the integrality constraints on $\mathbf{U}(k)$ and the expressions (20)-(23). As we are using the 1-norm in all cost expressions, this minimization problem amounts to solving a *Mixed-Integer Linear Program* (MILP) for which efficient solvers exist.

The finite-time optimal control problem posed above tries to capture the average switching frequency. Therefore, a long prediction interval is beneficial. The adverse influence of model uncertainties, measurement errors and noise in general becomes more and more apparent as the prediction interval is increased. Besides that, the computational complexity explodes. To account for that, we propose to use a rather long prediction *interval*, but a short prediction *horizon* N . This is achieved by finely sampling the prediction model with $25 \mu\text{s}$ only for the first steps, but more coarsely with a multiple of $25 \mu\text{s}$ for steps far in the future. Although this approach is similar to utilizing blocking control moves, using a coarsely sampled model proves to be advantageous in the hybrid domain reducing the complexity and thus the computation times. We call this approach the *Multiple Prediction Model Approach*, that leads to a time-varying prediction model.

V. SIMULATION RESULTS

The simulations were carried out using ABB's Matlab/Simulink model of the ACS6000 drive [5], where the look-up table with ABB's DTC strategy was replaced by a function solving at each time-step the optimal control problem online. The parameters of the drive can be found in [6]. The bounds for the torque and the stator flux depend on the operating point and are imposed by an outer control loop in the Matlab/Simulink model. A particularity of the specific inverter considered here is that restrictions on the switch transitions are present. These restrictions stem from technicalities regarding the construction of the inverter, and are easily taken into account in the Optimal DTC scheme by introducing additional constraints on the integer manipulated variables.

The optimal control problem was solved for the objective function (24) using a prediction horizon of $N = 4$. Employing the Multiple Prediction Model Approach, the first two steps were set equal to the sampling time of $25 \mu\text{s}$ and the remaining two were equal to $100 \mu\text{s}$. To allow for a comparison of ABB's DTC with the proposed Optimal DTC scheme, the penalties on the soft constraints were chosen such that the resulting ripples for the torque, flux and neutral point potential are the same. This led to $q_T = 800$ for the torque, $q_F = 700$ for the stator flux and $q_N = 4500$ for the neutral point potential. The switch transitions are penalized with $q_u(0) = 16$, exponentially decaying within the prediction horizon. The deviations from the references are penalized with $q_f = q_n = 0.04$ for the stator flux and the neutral point potential, respectively. The distribution

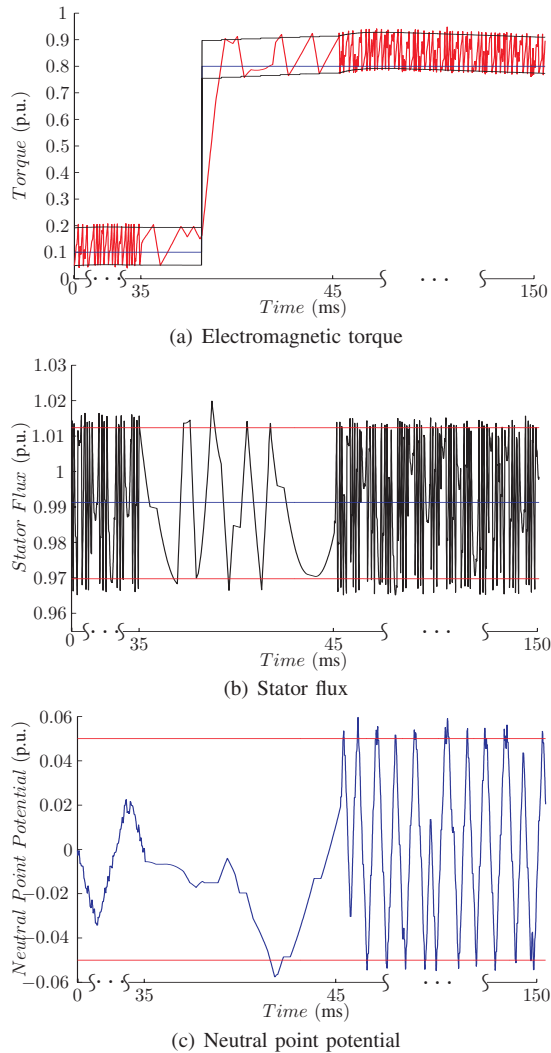


Fig. 3. Closed-loop simulation of the Optimal DTC scheme during a step change in the torque reference for a DTC drive with a three-level inverter

of the switching effort is enforced with $q_\lambda = 0.2$. The computation times required for the solution of the optimal control problem at each time-step were in the range of 100 ms running CPLEX [9] on a 2.8 GHz Pentium PC.

Initially, the motor is running with a speed of $\omega_r = 0.4$ p.u. under a load torque of $T_\ell = 0.1$ p.u., when a step in the torque reference $T_{e,ref}$ is applied from 0.1 p.u. to 0.8 p.u.. Fig. 3 depicts the closed-loop behavior of the torque, the stator flux and the neutral point potential under Optimal DTC. As can be seen, the Optimal DTC scheme preserves the rapid dynamic responses achieved by the classic DTC approach. The degree of the violation of the bounds is a design parameter adjustable by the penalties on the soft constraints. Most important, the average switching frequency for Optimal DTC is only 196 Hz compared to ABB's 256 Hz. This improvement amounts to a reduction of the average switching frequency in the range of 20%, which translates in an equivalent reduction of the switching losses.

VI. CONCLUSIONS AND OUTLOOK

The scope of this paper is the investigation of the potential improvements that can be achieved using MPC for the hybrid control problem of DTC. The most crucial ingredient for this is the derivation of a hybrid model of the DTC drive that is of low complexity but yet of sufficient accuracy, followed by the formulation of an optimal controller. The latter is tailored to the peculiarities of the DTC problem employing three different penalty levels, the late switching strategy and the multiple model approach. In particular, this control approach is based on a systematic design procedure allowing one to easily adapt it to other inverter topologies and induction motor characteristics. Furthermore, this approach clearly demonstrates the existing potential for performance improvement compared to state of the art industrial DTC look-up tables, as the comparison with ABB's ACS6000 drive shows.

However, the control actions are obtained by solving the optimization problem online. As the computation times well exceed the sampling time of DTC, the proposed controller cannot be directly implemented and experimentally verified making it mandatory to compute the (explicit) state-feedback control law leading to an optimal look-up table. For this, preliminary results have been obtained showing that the practical implementation of the Optimal DTC is within reach. An extended version of this paper, including the derivation of the state-feedback control law can be found in [6].

VII. ACKNOWLEDGEMENTS

This work was supported by ABB Switzerland Ltd., and by the IST research project IST-2001-33520 *Control and Computation* of the EU. The authors would like to thank Christian Stulz, Pieder Joerg and Petri Schroderus of ABB ATDD, Turgi, Switzerland, and Andreas Poncet of ABB Corporate Research, Baden-Dättwil, Switzerland, for their continuous advice.

REFERENCES

- [1] I. Takahashi and T. Noguchi. A New Quick Response and High Efficiency Control Strategy of an Induction Motor. *IEEE Trans. on Industry Applications*, 22(2), March/April 1986.
- [2] P. Tiitinen and M. Surandra. The Next Generation Motor Control Method, DTC Direct Torque Control. In *Proc. of the 1996 International Conf. on Power Electronics, Drives and Energy Systems for Industrial Growth*, volume 1.
- [3] A. Bemporad and M. Morari. Control of Systems Integrating Logic, Dynamics, and Constraints. *Automatica*, 35(3):407–427, March 1999.
- [4] M.L. Tyler and M. Morari. Propositional logic in control and monitoring problems. *Automatica*, 35(4):565–582, April 1999.
- [5] ABB Asea Brown Boveri Ltd. Product webpage of ACS 6000. online document. www.abb.com/motors&drives.
- [6] G. Papafotiou, T. Geyer, and M. Morari. Optimal direct torque control of three-phase symmetric induction motors. Technical Report AUT03-07, Automatic Control Laboratory ETH Zurich, <http://control.ee.ethz.ch>, 2003.
- [7] P. C. Krause. *Analysis of Electric Machinery*. McGraw-Hill, NY, 1986.
- [8] H. du Toit Mouton. Natural Balancing of Three-Level Neutral-Point-Clamped PWM Inverters. *IEEE Trans. on Industrial Electronics*, 49(5), October 2002.
- [9] ILOG, Inc. *CPLEX 8.0 User Manual*. Gentilly Cedex, France, 2002.